

Morphology control in synthesis of nickel nanoparticles in the presence of polyvinylpyrrolidone (PVPK30)

Dayong Liu · Shan Ren · Hui Wu · Qingtang Zhang · Lishi Wen

Received: 19 October 2007 / Accepted: 8 January 2008 / Published online: 1 February 2008
© Springer Science+Business Media, LLC 2008

Abstract Nickel nanoparticles with different morphologies have been synthesized with polyvinylpyrrolidone (PVPK30) as structure-directing agent through a chemical reduction process. SEM, TEM and selected-area electron diffraction (SAED) were employed in the analysis of morphological characteristics of nickel nanoparticles. It was found that nickel nanoparticles are formed by the aggregation of nanoscale nickel crystallites, and particle morphology was strongly dependent on the PVPK30 concentration. In addition, crystallite size and formation time of nickel nanoparticles increased with the increasing PVPK30 concentration. PVPK30 additive seems to influence the three steps of nickel particle precipitation: nucleation, crystal growth and aggregation. The resultant spherical nickel nanoparticles showed high coercivity.

Introduction

Synthesis of nickel nanoparticles has been studied extensively over the past decade due to their unique properties and applications in various fields, such as chemical catalysts, electrical conductive polymers, battery materials and nickel–ceramics complex, etc. [1–4]. Their electric and

magnetic properties are strongly dependent on the morphology and shape of nickel particles [5, 6]. Therefore, nickel nanoparticles with different morphology and shape, such as nanospheres, hollow sphere, nanorod, nanobelt and core-shell structure, have been synthesized by various methods [7–15]. In fact, nanometer-sized crystallites are often the primary product in precipitation from solution. Such dispersions are inherently unstable and the so-formed nanoscale crystallites aggregated to form larger particles. For example, different morphological copper oxalate particles aggregating different shape crystallites have been synthesized in the presence of hydroxypropylmethylcellulose (HPMC) [16], and they found that addition of different HPMC concentration induces different particles and crystallite morphology. Xiaomin Ni and co-workers have reported a chainlike nickel wire formed by self-assembly of small nickel crystallites in soft template [17]. To the best of our knowledge, however, little attention has been paid to investigate the morphology control of spherical nickel nanoparticles by altering the relative rate of nucleation and growth. The objective of this research is to control the morphology of nickel nanoparticles by tailing nucleation, crystal growth and aggregation process in presence of polyvinyl pyrrolidone (PVPK30) with different concentrations.

In this paper, spherical and aristate spherical nickel nanoparticles have been successfully synthesized with polyvinyl pyrrolidone (PVPK30) as a structure-directing agent through a chemical reduction process. Characterization of the precipitations was studied with SEM, TEM and XRD. Effect of PVPK30 concentration on the morphology, crystallite size and formation time of nickel nanoparticles was investigated. Influence of PVPK30 concentration on the nucleation growth and aggregation process of nickel crystallite was mainly discussed. In addition, magnetic

D. Liu · S. Ren (✉) · H. Wu · Q. Zhang · L. Wen
The Center for Nanotechnology Research, State Key Laboratory of Optoelectronic Material and Technologies, School of Physical Science and Technology, Sun Yat-Sen University, Guangzhou 510275, P.R. China
e-mail: stsr@s@mail.sysu.edu.cn

D. Liu
e-mail: liudayong1974@126.com

property of the aristate spherical nickel powders was also measured.

Experimental procedure

Nickel nanoparticles were prepared as follows: various amounts of PVPK30 (0.5 g, 2 g, 4 g, 10 g, $M_w = 40000$) and a suitable amount of palladium ions (Tedia, Japan) were added to 250 mL aqueous solution of 0.4 M NiCl_2 under stirring, 25 mL hydrazine hydrate ($\text{N}_2\text{H}_4 \cdot \text{H}_2\text{O}$, 50%) and 8 g NaOH were dissolved in 250 mL deionized water under stirring. The two solutions were mixed and heated to 60 °C by using hot water. The solution becomes black quickly, indicating that the nickel crystallite is forming. At the end of reaction, the black products were washed with distilled water and alcohol alternately for three times and dried at 50 °C in a vacuum oven.

Characterization of the nickel powders was performed by several techniques. The morphology and structure of product were characterized by scanning electron microscopy (JEOL, JSM-6330F), transmission electron morphology (JEOL, JEM-2010HR) and selected-area electron diffraction. The crystalline structure was identified using an X-ray diffractometer (D/Max-III, Rigaku, Japan, $\lambda_{\text{Cu-K}\alpha} = 1.5405 \text{ \AA}$). The magnetic hysteresis loops (M-H loops) of the nickel particles were recorded by a vibrating sample magnetometer (model MPMS XL-7).

Results and discussion

Morphology of the nickel nanoparticles was critically dependent on the PVPK30 concentration. Figure 1 presents the SEM image of a typical nickel particle prepared with 8 g/L PVPK30, which shows that all the products are aristate spherical nickel nanoparticles with an average diameter of 100 nm (see Fig. 1a). Ultra-fine structures of

the sample were further investigated by TEM and selected-area electron diffraction (SAED). It can be seen that many nano-sized nickel spikes, with length of 20–100 nm, were grown on the surface of nickel particles (see Fig. 1b). The SAED pattern (upper inset, Fig. 1b) demonstrates that the synthesized nickel particles are nickel polycrystalline, indicating nickel particles were formed by the aggregation of nickel crystallites. The SAED pattern (lower inset in Fig. 1b) of a single nickel spike demonstrates that nano-sized spikes were single crystallites, and it can be indexed to be [001] zone axis of fcc nickel.

Figure 2 presents SEM images of nickel nanoparticles prepared with different PVPK30 concentrations. When the PVPK30 concentration was 1 g/L, all the products were spherical nanoparticles with a mean diameter of 60 nm (Fig. 2a). Nickel powders switched to aristate spherical nanoparticles as PVPK30 concentration increases to 4 g/L and 8 g/L (Fig. 2b and fig. 1a). However, nickel particles change to a sphere again as PVPK30 concentration increased to 20 g/L. It is obvious that PVPK30 concentration plays an important role in determining the morphology of nickel particles.

Figure 3 shows the XRD pattern of the nickel nanoparticles prepared with different PVPK30 concentrations. All diffraction peaks of the samples could be indexed to the face centred cubic phase of nickel (J CPDS. No 0420860), indicating all the nickel salts were reduced to nickel metal. From the full width at half maximum of (111) peak, the mean grain sizes of the four samples prepared with 1 g/L PVPK30, 4 g/L PVPK30, 8 g/L PVPK30 and 20 g/L PVPK30 were calculated to be 15.6, 16.3, 17.0 and 17.9 nm, respectively. The crystallite size of all the nickel nanoparticles is much smaller than the diameter of the nickel particles, which suggests the nickel nanoparticles were formed by the aggregation of nickel crystallites, consistent with SAED results.

PVPK30 concentration has a great influence on the crystallite size and formation time of nickel nanoparticles.

Fig. 1 (a) SEM images, and (b) TEM images of aristate spherical nickel nanoparticles prepared with 8 g/L PVPK30 (inset in Fig. 1b is the SAED patterns of nickel particles and single nickel spike)

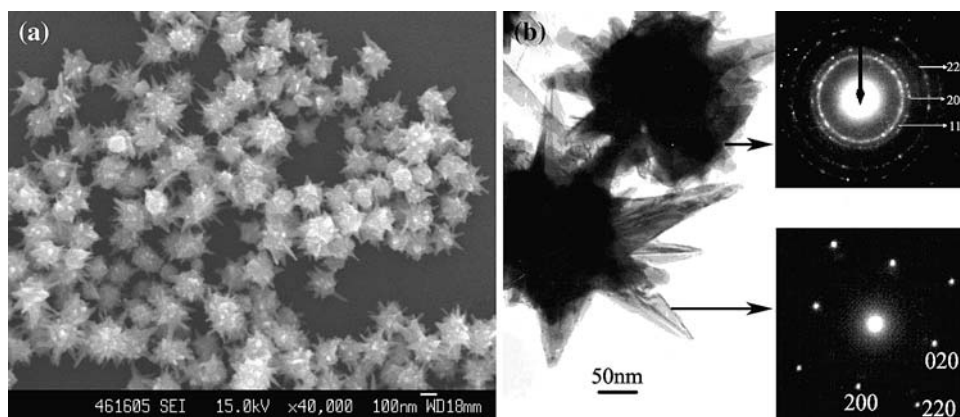


Fig. 2 SEM images of nickel nanoparticles prepared with different PVPK30 concentrations: (a) 1 g/L, (b) 4 g/L, (c) 20 g/L

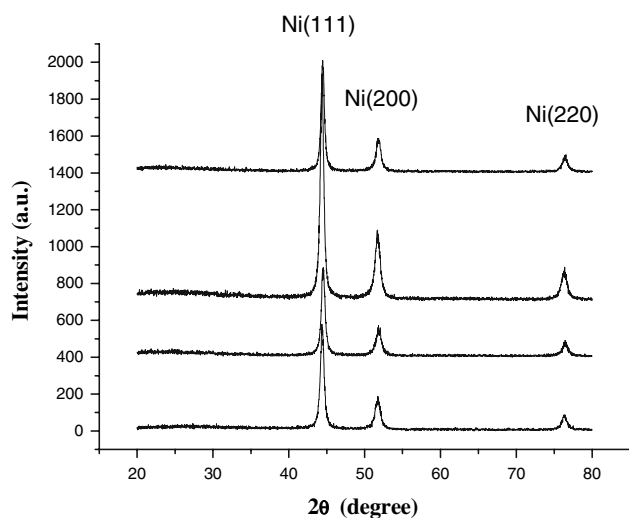
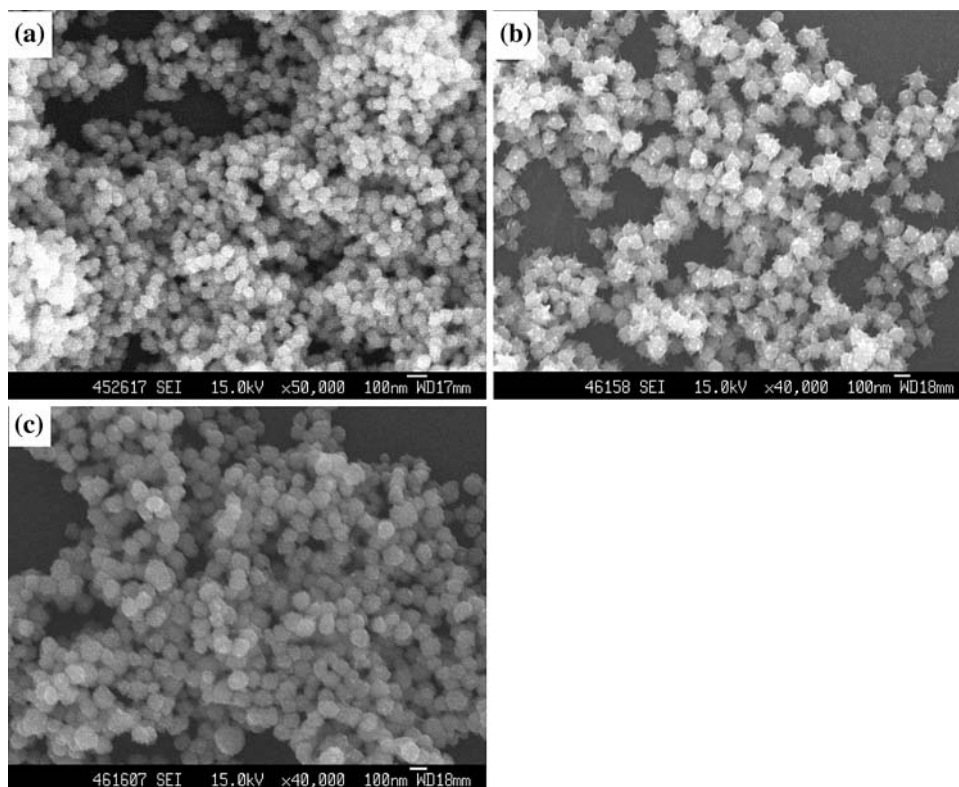


Fig. 3 XRD pattern of the nickel nanoparticles prepared with different PVPK30 concentrations: (a) 1 g/L, (b) 4 g/L, (c) 8 g/L, (d) 20 g/L

It should be pointed out that formation time is the period from the mixing of all the reagents to the end of the reaction. Effect of PVPK30 concentration on the nickel crystallite size and formation time of nickel nanoparticles is presented in Fig. 4. It can be seen that both crystallite sizes and formation time of nickel nanoparticles increase with the increase of PVPK30 concentration.

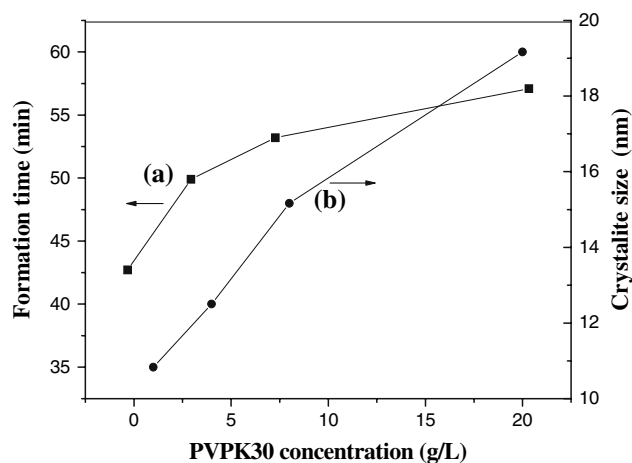


Fig. 4 Effects of PVPK30 concentration on the (a) formation time and (b) crystallite size of nickel nanoparticles

We will now discuss the influence of PVPK30 molecule on the nucleation, growth and aggregation of the nickel crystallite which may help to understand the effect of PVPK30 concentration on the formation time, crystallites size and shape of nickel nanoparticles. Earlier research works have proved that PVP molecule could coordinate with metal ions to form stable metal–PVP complex by FT-IR spectrometry [18, 19]. It is obvious that the reduction rate of nickel–PVP complex will be lower than that of NiCl₂

or $\text{Ni}(\text{OH})_2$, which inevitably increases the time for nickel atoms reaching supersaturation. Therefore, we believe that the nucleation rate of nickel crystallite decreased with increasing PVPK30 concentration. Moreover, growth rate of nickel crystallite will decrease as its face was adsorbed PVPK30 molecules, because crystal growth rate is generally lowered with adsorbed polymer [20]. As a result, formation time of nickel nanoparticles increases with the increasing PVPK30 concentration. It seems that crystallite size should be decreased with the increasing PVPK30 concentration due to the lower growth rate of nickel crystallite. On the contrary, crystallite size increases with the increasing PVPK30 concentration, which possibly contributes to the longer period for crystal growth.

Morphology of the nickel nanoparticles was critically dependent on the PVPK30 concentration. We believe that one of the key factors in explaining shape alteration of nickel particles is the difference in the crystal growth in different directions. It is known that crystal growth rate generally decreased with the adsorbed polymer, and crystallite morphology can be altered by the presence of polymer specifically interacting with crystal faces [21]. Nickel nanoparticles are spherical as PVP concentration is low (1 g/L), because there are not enough PVPK30 molecules adsorbed on the face of the nickel crystallite to alter the growth rate in different directions. That is to say, growth rate of the spherical nickel crystallite in all the directions is the same. Therefore, nickel crystallite will grow up to a spherical crystallite, followed by the aggregation of the crystallites to form the spherical nickel nanoparticles. When the PVPK30 concentration is proper (4 g/L and 8 g/L), growth rate of the face adsorbed PVPK30 molecule is lower than that of face without PVPK30 molecule. As a result, nickel crystallite will grow up to a rod crystallite, then, aristate spherical nickel nanoparticles are formed by the aggregation of the rod crystallites. Products change to spherical nickel nanoparticles again as PVP concentration is too high (20 g/L); we assume that growth rate of crystallite in all the directions is also the same because all the faces of nickel crystallites are adsorbed by the PVPK30 molecule.

Magnetic measurements on the aristate spherical nickel nanoparticles were conducted. Figure 5 presents the M-H hysteresis loop measured at room temperature, which shows that coercivity (H_c), saturation (M_s) and remanent magnetization (M_r) values of the sample are ca. 304 Oe, 52.5 and 9.6 emu/g, respectively. Compared with that of the bulk nickel ($H_c = 100$ Oe, $M_s = 55$ emu/g), aristate spherical nickel nanoparticles exhibited increased coercivity. Due to the magnetic properties of nanoparticles, closely associated with their small size and microstructure, we believe that the nanoscale nickel crystallite and novel morphology of the particle contribute to the high coercivity

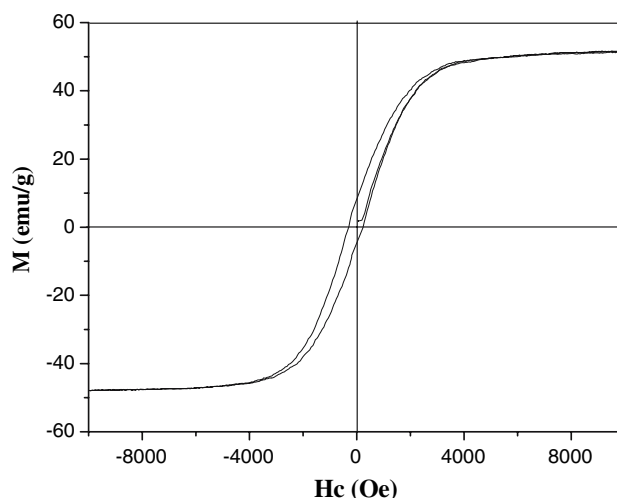


Fig. 5 M-H loop of the aristate spherical nickel nanoparticles prepared with 8 g/L PVPK30

[22]. In addition, the M_s value was reduced relative to that of the bulk nickel, which was possibly resulted from the spin disorder in the interface of nickel crystallite.

Conclusions

Aristate spherical and spherical nickel nanoparticles were synthesized with polyvinyl pyrrolidone (PVPK30) as a structure-directing agent through a chemical reduction process. Nickel nanoparticles were formed by the aggregation of nanoscale nickel crystallites. Formation of aristate spherical nickel nanoparticles was critically dependent on PVPK30 concentration. In addition, formation time and crystallite size increased with the increasing PVPK30 concentration. The PVPK30 additive seems to influence the three steps of nickel nanoparticle precipitation: nucleation, crystal growth and aggregation. These resultant aristate spherical nickel nanoparticles with high coercivity could be used as excellent high density magnetic recording materials.

Acknowledgements This research was financially supported by both the Science & Technology project of Guangzhou city and the Science & Technology Department of Guangdong Province, China.

References

1. Duan YW, Li JG (2004) Mater Chem Phys 87:452
2. Hirai H, Yakura N (2001) Polym Adv Technol 12:724
3. Levi G, Scheu C, Kaplan WD (2001) Interf Sci 9:213
4. Lee JY, Lee JH, Hong SH, Lee YK, Choi JY (2003) Adv Mater 15:1655
5. Kim KH, Lee YB, Choi EY, Park HC, Park SS (2004) Mater Chem Phys 86:420

6. Cordente N, Respaud M, Senocq F, Casanove MJ, Amiens C, Chaudret B (2001) *Nano Lett* 1:565
7. Franquin D, Monteverdi S, Molina S, Bettahar MM, Fort Y (1999) *J Mater Sci* 34:4481. doi:[10.1023/A:1004637221636](https://doi.org/10.1023/A:1004637221636)
8. Chou KS, Huang KC (2001) *J Nanoparticles Res* 3:127
9. Kim KH, Lee YB, Lee SG, Park HC, Park SS (2004) *Mater Sci Eng A* 381:337
10. Kurinec SK, Okeke N, Gupta SK, Zhang H, Xiao TD (2006) *J Mater Sci* 41:8181. doi:[10.1007/s10853-006-0393-0](https://doi.org/10.1007/s10853-006-0393-0)
11. Yu KN, Kim DJ, Chung HS, Liang HZ (2003) *Mater Lett* 57:3992
12. Couto GG, Klein JJ, Schreiner WH, Mosca DH, de Oliveira AJA, Zarbin AJG (2007) *J Colloid Interf Sci* 311:461
13. Ni XM, Zhao QB, Zhang DG, Yang DD, Zheng HG (2005) *J Cryst Growth* 280:217
14. Li D, Komarneni S (2006) *J Am Ceram Soc* 89:1510
15. Bao J, Liang Y, Xu Z, Si L (2003) *Adv Mater* 15:1832
16. Jongen N, Bowen P, Lemaitre J, Valmalette JC, Hofmann H (2000) *J Colloid Interf Sci* 226:189
17. Ni XM, Zhang YF, Song JM, Zheng HG (2007) *J Cryst Growth* 299:365
18. Zhang ZT, Zhao B, Hu LM (1996) *J Solid State Chem* 121:105
19. Rivas BL, Pereira ED, Villoslada IM (2003) *Prog Polym Sci* 28:173
20. Van der Put PJ (1998) In: *The inorganic chemistry of materials: how to make things out of elements*. Plenum, New York, pp 278
21. Sun YG, Xia YN (2002) *Science* 298:2176
22. Yoon M, Kim Y, Kim YM, Volkov V, Song HJ, Park YJ, Park I-W (2005) *Mater Chem Phys* 91:104